Supplementary information

Enzyme purification improves the enzyme loading, self-propulsion and endurance performance of micromotors

Morgane Valles,[†] *Sílvia Pujals,*[†] *Lorenzo Albertazzi,*[†,‡] *Samuel Sánchez*[*,†,§]

[†]Institute for Bioengineering of Catalonia (IBEC), The Barcelona Institute of Science and Technology (BIST), Baldiri i Reixac 10-12, 08028 Barcelona, Spain

[‡] Department of Biomedical Engineering, Institute for Complex Molecular Systems (ICMS), Eindhoven University of Technology, 5612AZ Eindhoven, The Netherlands

[§]Institució Catalana de Recerca i Estudis Avançats (ICREA), Pg. Lluís Companys 23, 08010 Barcelona, Spain

Content:

Supplementary Figures

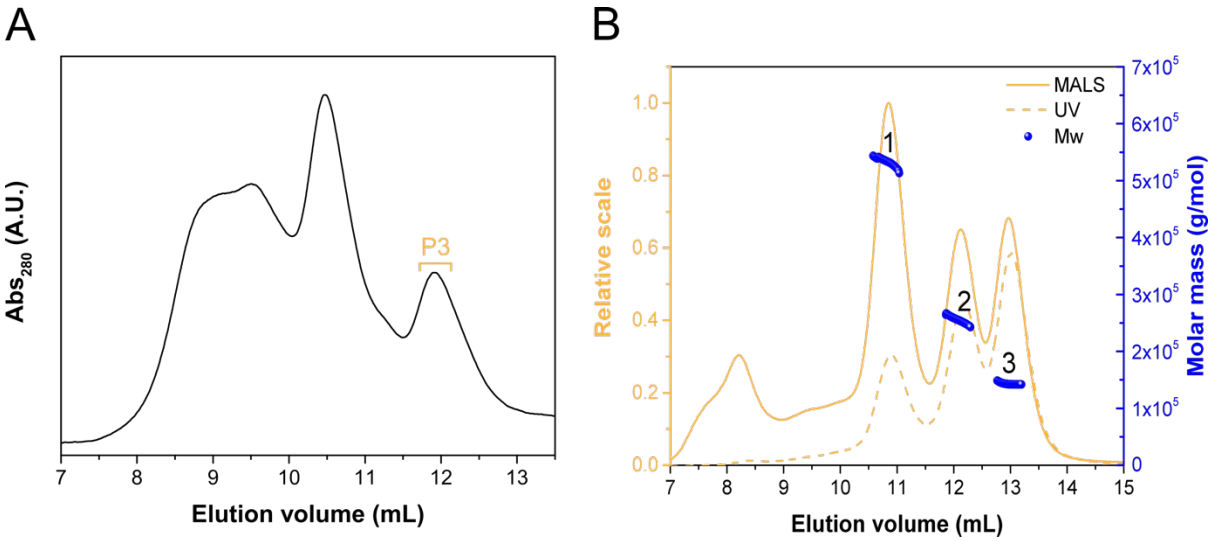

Figure S1 Analysis of the P3 SEC peak by SEC-MALS. **(A)** Chromatogram from size-exclusion run on Urease type IX using a Bio-rad ENrich SEC 650 10 x 300 column. The third peak (P3) was analysed by SEC-MALS. **(B)** SEC-MALS analysis of P3 in (A) showing 3 peaks of distinct molecular weights (Mw). The MALS curve is represented by a solid orange line, the absorbance at 280 nm (UV) detected during the SEC is represented by a dashed line, and measured molecular weight of the eluted protein found in each peak is represented by blue spheres. More information about the SEC-MALS peaks can be found in **Table S1**.

Table S1 Molar mass estimates of the peaks from the SEC-MALS run on P3, as determined using the ASTRA7 analysis software

Peak	Mn (kDa)	Mw (kDa)	Polydispersity (Mw/Mn)	Calculated mass (µg)	Mass fraction (%)

Peak 1	532.45 ± 5.62	532.55 ± 5.62	1.00 ± 0.1	15.02	21.11
Peak 2	254.20 ± 2.72	254.35 ± 2.73	1.00 ± 0.02	8.03	27.49
Peak 3	143.03 ± 1.57	143.05 ± 1.57	1.00 ± 0.02	6.17	51.41

Table S2 Kinetic parameters of each peak found in the size-exclusion purification of urease type IX

Kinetic parameters	**P1**	**P2 (Ur-hex)**	**P3 (Ur-imp)**
V_{max} **(µM/s)**	0.676 ± 0.031	0.7109 ± 0.037	0.2989 ± 0.024
K_M **(mM)**	1.748 ± 0.552	2.06 ± 0.719	0.7083 ± 0.511
k_{cat} **(s^{-1})***	1,352 ± 61.288	1,421.4± 74.169	597.8 ± 48.434
k_{cat}/K_M	773.46	690.67	843.99

* determined by dividing the V_{max} by the concentration of urease used for assays (0.5 nM).

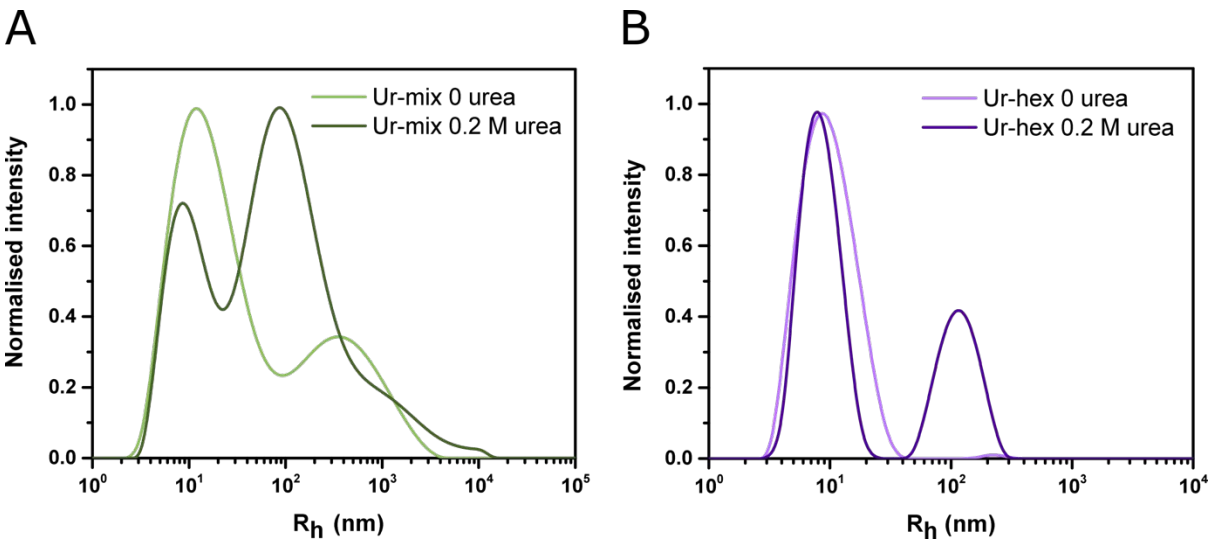

Figure S2 Distribution of hydrodynamic radii of protein species found in Ur-mix (A) and Ur-hex (B) samples in the absence and presence of 0.2 M urea, as measured by DLS.

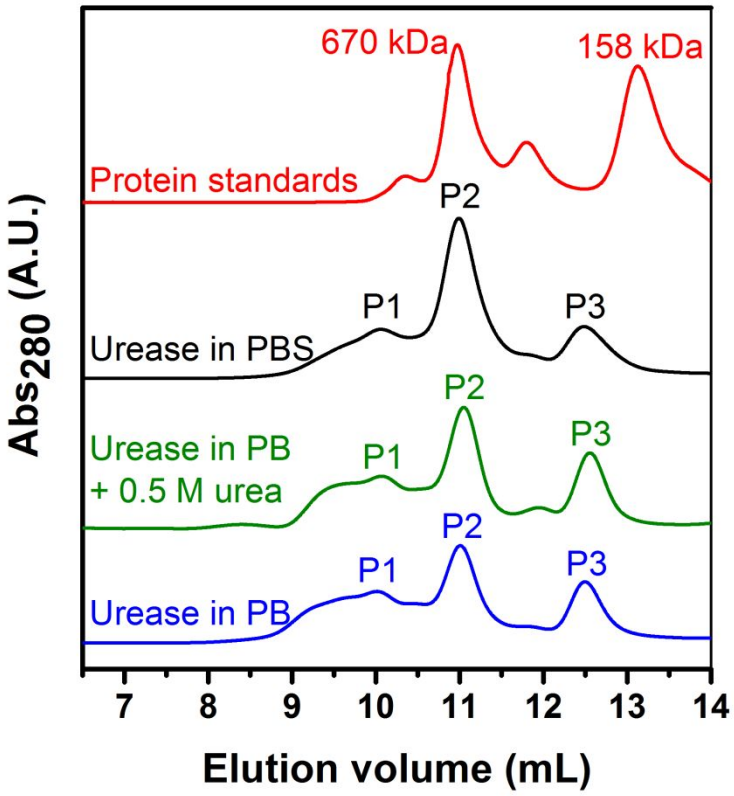

Figure S3 Chromatograms from the size-exclusion chromatography of urease in PBS (black), urease in phosphate buffer (PB) with 0.5 M urea added to the sample (green) and urease in PB (blue). The protein standards (red) show the elution volume of thyroglobulin (670 kDa) and gamma globulin (158 kDa).

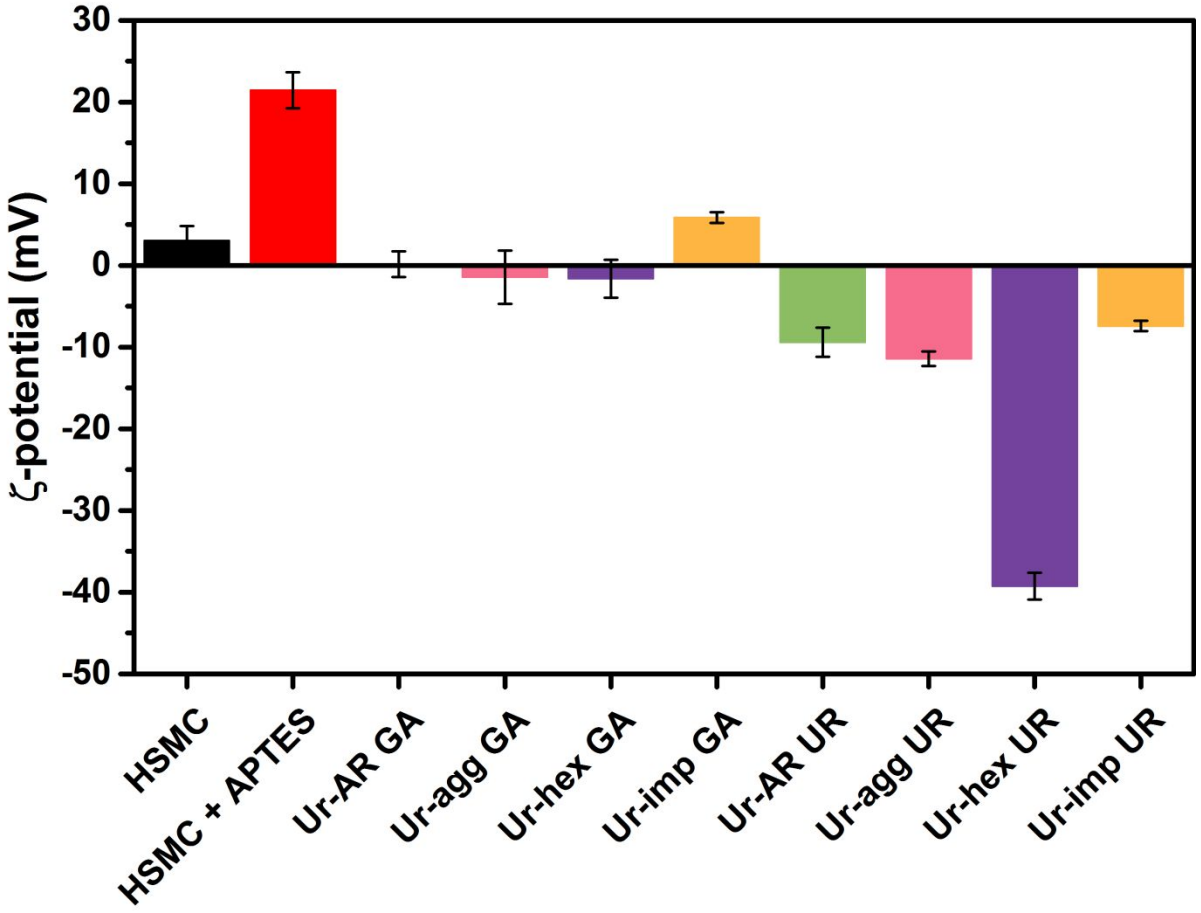

Figure S4 Zeta potential of the urease micromotors at various stages of functionalisation

Table S3 Biophysical properties of protein species described in this work, computed using protparam.

Properties	**Urease**	**Canavalin**	**Bovine serum albumin**
Molecular mass (kDa)	544.396	150.944	69.593
Isoelectric point (pI)	6.06	5.44	5.82
Lysine content (%)	6.0	4.5	9.9
Hydropathicity (GRAVY)	-0.152	-0.443	-0.429

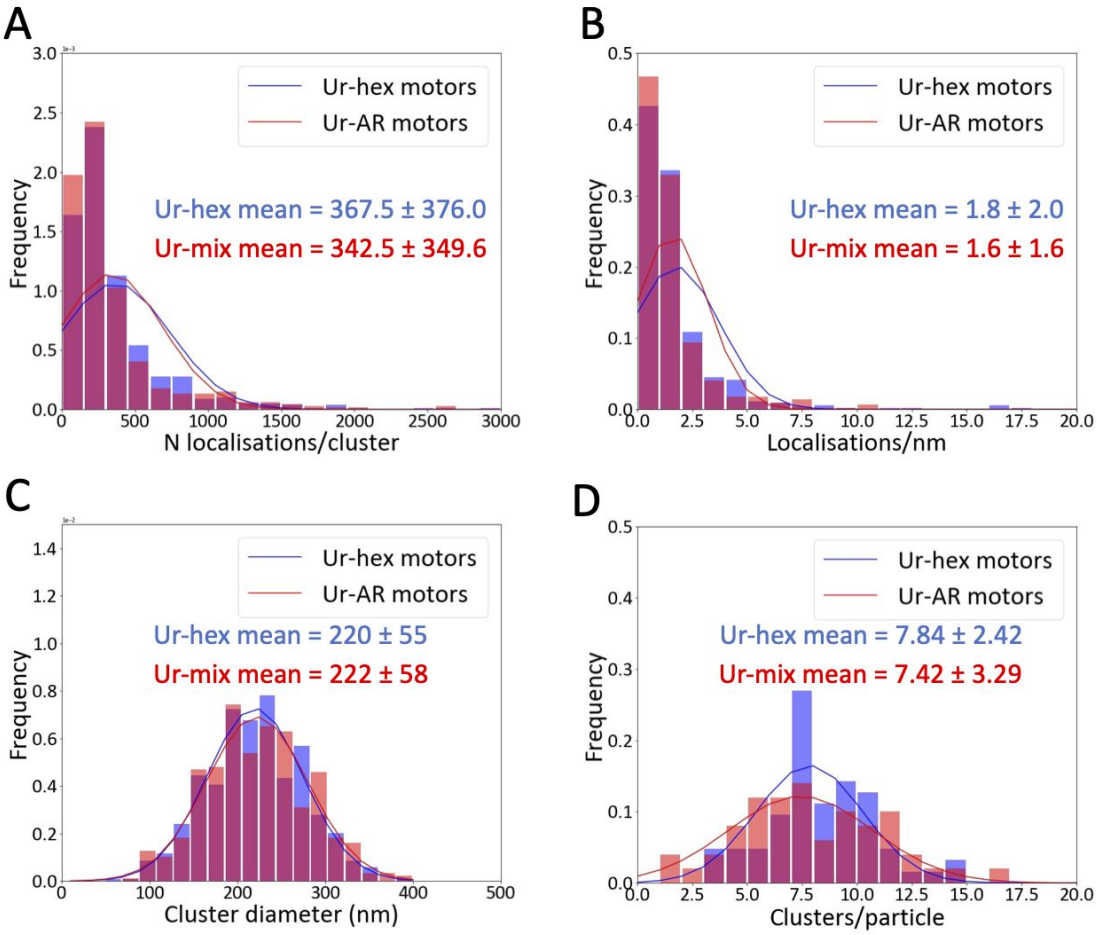

Figure S5 Analysis of the clusters found on the surface of the urease motors imaged by STORM. Histograms and associated distribution curves showing the sizes (in number of localisations per cluster, panel A), density (in localisations per nm, panel B), and diameters (panel C) of the clusters found on the surface of the Ur-hex (blue) and Ur-AR (red) motors, as well as the number of clusters found per particle (panel D).

References

(1) Patton, C. J.; Crouch, S. R. Spectrophotometric and Kinetics Investigation of the Berthelot Reaction for the Determination of Ammonia. *Anal. Chem.* **1977**, *49* (3), 464–469. DOI:10.1021/ac50011a034.

(2) Riedel, C.; Gabizon, R.; Wilson, C. A. M.; Hamadani, K.; Tsekouras, K.; Marqusee, S.; Pressé, S.; Bustamante, C. The Heat Released during Catalytic Turnover Enhances the Diffusion of an Enzyme. *Nature* **2015**, *517* (7533), 227–230. DOI:10.1038/nature14043.

(3) Patiño, T.; Feiner-Gracia, N.; Arqué, X.; Miguel-López, A.; Jannasch, A.; Stumpp, T.; Schäffer, E.; Albertazzi, L.; Sánchez, S. Influence of Enzyme Quantity and Distribution on the Self-Propulsion of Non-Janus Urease-Powered Micromotors. *J. Am. Chem. Soc.* **2018**, *140* (25), 7896–7903. DOI:10.1021/jacs.8b03460.

(4) Arqué, X.; Romero-Rivera, A.; Feixas, F.; Patiño, T.; Osuna, S.; Sánchez, S. Intrinsic Enzymatic Properties Modulate the Self-Propulsion of Micromotors. *Nat. Commun.* **2019**, *10* (1), 2826. DOI:10.1038/s41467-019-10726-8.

(5) Patino, T.; Porchetta, A.; Jannasch, A.; Lladó, A.; Stumpp, T.; Schäffer, E.; Ricci, F.; Sánchez, S. Self-Sensing Enzyme-Powered Micromotors Equipped with PH-Responsive DNA Nanoswitches. *Nano Lett.* **2019**, *19* (6), 3440–3447. DOI:10.1021/acs.nanolett.8b04794.

(6) Dunderdale, G.; Ebbens, S.; Fairclough, P.; Howse, J. Importance of Particle Tracking and Calculating the Mean-Squared Displacement in Distinguishing Nanopropulsion from Other Processes. *Langmuir* **2012**, *28* (30), 10997–11006. DOI:10.1021/la301370y.

(7) Howse, J. R.; Jones, R. A. L.; Ryan, A. J.; Gough, T.; Vafabakhsh, R.; Golestanian, R. Self-Motile Colloidal Particles: From Directed Propulsion to Random Walk. *Phys. Rev. Lett.* **2007**, *99* (4), 48102. DOI:10.1103/PhysRevLett.99.048102.

(8) Mestre, R.; Palacios, L. S.; Miguel-López, A.; Arqué, X.; Pagonabarraga, I.; Sánchez, S. Extraction of the Propulsive Speed of Catalytic Nano- and Micro-Motors under Different Motion Dynamics. **2020**, 1–18.

(9) Gasteiger, E.; Hoogland, C.; Gattiker, A.; Duvaud, S.; Wilkins, M. R.; Appel, R. D.; Bairoch, A. Protein Identification and Analysis Tools on the ExPASy Server. In *The Proteomics Protocols Handbook*; Walker, J. M., Ed.; Humana Press: Totowa, NJ, 2005; pp 571–607. DOI:10.1385/1-59259-890-0:571.

(10) Patiño, T.; Llacer-wintle, J.; Pujals, S.; Albertazzi, L.; Sánchez, S. Protein Corona Formation around Biocatalytic Nanomotors Unveiled by STORM. *Chemrxiv* **2021**, 16–19. DOI:10.33774/chemrxiv-2021-rhtps.

(11) Delcanale, P.; Albertazzi, L. DNA-PAINT Super-Resolution Imaging Data of Surface Exposed Active Sites on Particles. *Data Br.* **2020**, *30*, 105468. DOI:10.1016/j.dib.2020.105468.